Journal of Atmospheric and Solar-Terrestrial Physics 182 (2019) 31–38

Contents lists available at ScienceDirect

Journal of Atmospheric and Solar-Terrestrial Physics

journal homepage: www.elsevier.com/locate/jastp

Has global warming already arrived?

C.A. Varotsos*, M.N. Efstathiou

Climate Research Group, Division of Environmental Physics and Meteorology, Faculty of Physics, National and Kapodistrian University of Athens, University Campus Bldg. Phys. V, Athens, 15784, Greece

ARTICLE INFO

Keywords:
Troposphere
Stratosphere
Power-law
Satellite observations
Climate components

ABSTRACT

The enhancement of the atmospheric greenhouse effect due to the increase in the atmospheric greenhouse gases is often considered as responsible for global warming (known as greenhouse hypothesis of global warming). In this context, the temperature field of global troposphere and lower stratosphere over the period 12/1978–07/2018 is explored using the recent Version 6 of the UAH MSU/AMSU global satellite temperature dataset. Our analysis did not show a consistent warming with gradual increase from low to high latitudes in both hemispheres, as it should be from the global warming theory. In addition, in the lower stratosphere the temperature cooling over both poles is lower than that over tropics and extratropics. To study further the thermal field variability we investigated the long-range correlations throughout the global lower troposphere-lower stratosphere region. The results show that the temperature field displays power-law behaviour that becomes stronger by going from the lower troposphere to the tropopause.This power-law behaviour suggests that the fluctuations in global tropospheric temperature at short intervals are positively correlated with those at longer intervals in a power-law manner. The latter, however, does not apply to global temperature in the lower stratosphere. This suggests that the investigated intrinsic properties of the lower stratospheric temperature are not related to those of the troposphere, as is expected by the global warming theory.

1. Introduction

Over the last decades, the rise in surface air temperature in regions of our planet has led to a debate in the scientific community about the causes and impacts of this temperature rise, especially if it comes from anthropogenic activities or is of natural origin.

We must bear in mind that by definition the climate system is part of the wider global system. In particular, it is composed of five subsystems the atmosphere, the cryosphere, the hydrosphere, the biosphere and the lithosphere, which interact with each other with mostly non-linear processes in space and time (e.g., IPCC, 2014; Lovejoy and Varotsos, 2016). Therefore, a change in a parameter of a climatic subsystem (e.g., atmospheric temperature) does not predict a climate change, as all other parameters of the atmosphere but also of other subsystems (known and measurable or not) are not necessarily known and stable.

Also, by definition, the climate is a complicated (displaying many degrees of freedom) and a complex (non-linear, dynamical, sensitive) system (e.g. Lucarini, 2011). Therefore, it is a truism that climate has always been changing, and it will always be changing. Which subsystem dominates the climate change depends, for instance, on the time window, namely: For $t < 10$yrs the atmospheric degrees of freedom are active and the other sub-systems are frozen. For $100 < t < 1000$yrs the ocean dominates, and for $t > 5000$yrs cryosphere dominates.

Several analyses have been made on the key issues of scientific understanding of contemporary global climate change (e.g. Christy et al., 2007). The focus of most of these analyses is to discuss the uncertainties associated with existing observation data and the results of numerical modelling. These emphasize the need to analyze the ability of current models to simulate real climate change. As mentioned above, real climate change results from the non-linear interactions between numerous components of the climatic system. In these should also be taken into consideration and possible contributions by external forcings e.g., cosmic factors, such as solar activity. Despite the projected exponential growth in computer power, these processes will not be adequately resolved in numerical climate models in the near future (Franzke et al., 2015). Stochastic methods for numerical climate prediction may allow for an adequate representation of uncertainties, the reduction of systematic biases and improved representation of long-term climate variability (e.g., Droegemeier, 2009). Some analyses show that current models are not able to simulate real climate. The main reason is that climate is a high-dimensional forced and dissipative complex system with chaotic dynamics that displays different physical and chemical properties of its various components and coupling

* Corresponding author.
E-mail address: covar@phys.uoa.gr (C.A. Varotsos).

https://doi.org/10.1016/j.jastp.2018.10.020
Received 1 September 2018; Received in revised form 29 September 2018; Accepted 29 October 2018
Available online 30 October 2018
1364-6826/

mechanisms. Furthermore, the understanding of slow and rapid extreme climatic events and the assessment of processes behind the tipping points responsible for the multi-stability of the climatic system is not complete (Lenton et al., 2008; Varotsos, 2002, 2013; Varotsos and Cartalis, 1991).

Lucarini et al. (2014) discussed several ideas from the basic physics that came into the climate science. For example, the powerful formulation of hydrodynamics based on formalism introduced by Nambu (1973) helps elucidate the hidden properties of fluid flows, leading to a new generation of numerical climate models. Another example, is the effort to build tools for the assessment of energy budget and transport and to study irreversible processes (by evaluating entropy production) through classical non-equilibrium thermodynamics and based on the views of Prigogine (1961) and of Lorenz (1967). Finally, efforts were made to employ the non-equilibrium statistical mechanics formulation of climate dynamics to address the climatic response to perturbations, based on the work of Ruelle (1997).

One aspect of the climate system, which is a matter of great concern to the international scientific community but also to humanity, is the so-called global warming. This is one of the components of global climate change and interconnected to human activity.

This is today a major challenge for mankind, with public debates on whether global warming is happening, how much has happened in modern times, whether action should be taken to combat it and, if so, what should be that action. It is often associated with, for example, rising sea level and decline in the Arctic sea ice. The increase in extreme events is also considered as a result of global warming (e.g. OGorman, 2014) and may have a wide and varied impact on health, agriculture and economics (Schleussner et al., 2016; Carleton and Hsiang, 2016). However, the detection of climate change and quantification of the enhancement of the atmospheric greenhouse effect, both in observations and in climate models, is the main concern of the scientific community (Kondratyev and Varotsos, 1995).

The purpose of the present study is to explore the temporal variability of the temperature on a global, hemispheric and latitudinal belt basis for the regions: lower troposphere, middle troposhere, tropopause and lower stratosphere using the Version 6 of the UAH MSU/AMSU global satellite temperature data set and to address the question whether the so-called global warming has already arrived.

2. Data and analysis

The present analysis attempts to explore the temperature field of the global troposphere and lower stratosphere over the period 12/1978–07/2018, using the recently released Version 6 of the UAH MSU/AMSU global satellite temperature dataset of NOAA (National Oceanic and Atmospheric Administration). Mean monthly values of temperature anomalies (departures from 30-year calendar monthly means, 1981–2010) were employed over tropics, extra-tropics and polar regions of both hemispheres, throughout the lower troposphere – lower stratosphere region (http://vortex.nsstc.uah.edu/data/msu/v6.0/tlt/uahncdc_lt_6.0.txt).

Linear regression analysis was used for the trend estimation of temperature anomalies (TA) time series. The statistical significance of the regression coefficients (i.e. the slope m, the y-intercept and the coefficient of determination R^2) was tested by using the t-test and F-test at a 95% confidence level.

To detect long-range correlations and multifractal properties of TA time series, detrended fluctuation analysis (DFA) and the multifractal detrended fluctuation analysis (MF-DFA) were employed (Varotsos, 2005; Varotsos et al., 2007, 2013a,b; Efstathiou and Varotsos, 2010, 2012, 2013; Peng et al., 1994; Weber and Talkner, 2011; Kantelhardt et al., 2002).

The basic steps of the MF-DFA technique are given below:

1. We integrate the time series $x(i)$ over time by calculating the differences of the N observations $x(i)$ from their mean value x_{ave}, i.e. $x(i)$ - x_{ave}
2. We divide the integrated time series, $y(i)$, into non-overlapping segments of equal length, τ and we repeat the same procedure starting from the end of the profile, obtaining thus $2N_\tau$ segments (where N_τ is the integer part of the number N/τ).
3. We calculate the locally best polynomial fitted trend (of order l) in each segment and the corresponding variance, which is obtained by the types:
   a. For each segment $k = 1, \ldots, N_\tau$:

$$F^2(k,\tau) = \frac{1}{\tau}\sum_{i=1}^{\tau}[y((k-1)\tau + i) - z](i)^2 \quad (1)$$

   b. For each segment $k = N_\tau + 1, \ldots, 2N_\tau$:

$$F^2(k,\tau) = \frac{1}{\tau}\sum_{i=1}^{\tau}[y((N-k-N_\tau)\tau + i) - z](i)^2 \quad (2)$$

where $z(i)$ is a polynomial least-square fit to the τ data.

4. We estimate the q-th order fluctuation function by averaging the variances over all segments:

$$F_q(\tau) = \left[\frac{1}{2N_\tau}\sum_{k=1}^{2N_\tau}[F^2(k,\tau)]^{q/2}\right]^{1/q} \quad (3)$$

where q is the variable moment.

It is worth noting that in case of $q \to 0$, the Eq. (3) assumes the form:

$$F_o(\tau) = \exp\left[\frac{1}{2N_\tau}\sum_{k=1}^{2N_\tau} In[F^2(k,\tau)]\right]$$

5. We depict $F_q(\tau)$ vs. τ (in log-log plot) for different values of q and in case of multi-scaling behavior, a power-law behavior for $F_q(\tau)$ is observed:

$$F_q(\tau) \sim \tau^{h(q)} \quad (4)$$

where $h(q)$ is the generalized Hurst exponent which denotes the slope of the corresponding regression line.

MFDFA is derived from the original DFA, which estimates the monofractal scaling features of a time series (Peng et al., 1994). More precisely, the DFA fluctuation function $F_d(\tau)$ is computed by the Eq. (3) for $q = 2$ (without repeating the procedure starting from the end of the profile, i.e. $F_d(\tau) = \left[\frac{1}{N_\tau}\sum_{k=1}^{N_\tau}[F^2(k,\tau)]\right]^{1/2}$, where $F^2(k,\tau)$ is given by Eq. (1)).

For fractal series, a power-law behavior of $F_d(\tau)$ (i.e. $F_d(\tau) \sim \tau^{\alpha}$) characterized by the monofractal exponent α is expected. In particular, for $\alpha = 0.5$ the series is white noise, for $\alpha = 1$, the series is the so-called 1/f noise, for $0 < \alpha < 0.5$ the series presents power-law anticorrelations (antipersistence), while a value of α-exponent between 0.5 and 1.5 indicates long-range power-law correlations (persistence). In other words, the single fractal DFA-exponent α assumes that the fractal properties are homogeneous over all scales of the entire time series. The successive steps of the MF-DFA and DFA procedures are described in detail in Kantelhardt et al. (2002) and Varotsos et al. (2018), respectively.

The two techniques described above (DFA and MF-DFA) were applied on the detrended and deseasonalised TA time series. The detrending and the deseasonalisation were achieved by using linear or polynomial (of 6th order) best fit and the classical Wiener filter, respectively (Wiener, 1950).

Finally, to establish the long-range correlations in the TA time series we examined the two criteria proposed by Maraun et al. (2004) (i.e. the rejection of the exponential decay of the autocorrelation function and the existence of constancy for the "local slopes" $\alpha(\tau)$ of $\log F_d(\tau)$ vs. $\log \tau$

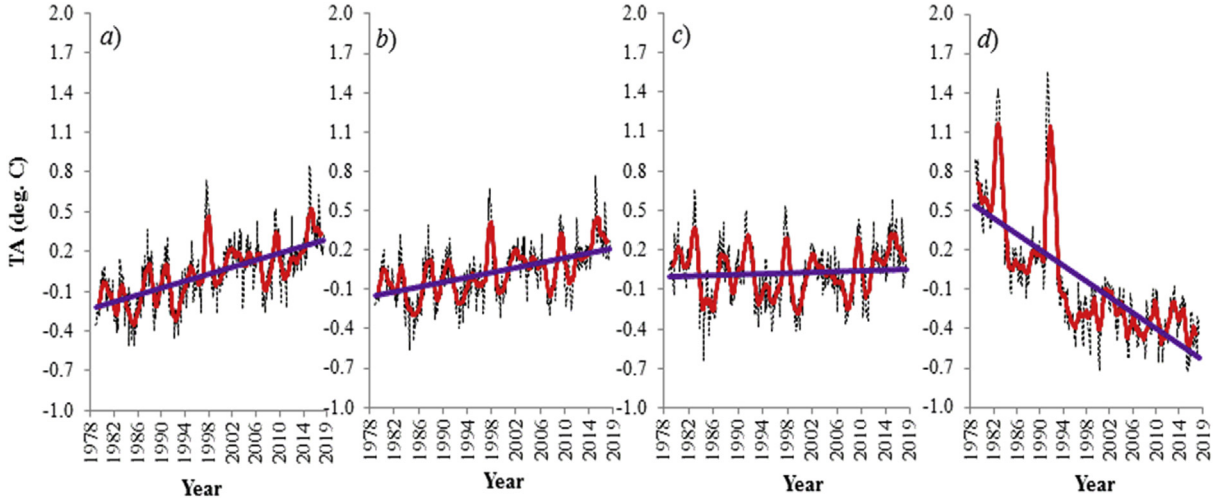

Fig. 1. Mean monthly values of the global area-averaged TA (departures from 30-year calendar monthly means, 1981–2010), for the period 12/1978–07/2018 (dotted black line) and the corresponding linear trend (blue solid line) and 13-month moving average (red solid line) for (a) the lower troposphere (0.13 °C/decade), (b) the mid-troposphere (0.09 °C/decade), (c) the tropopause (0.01 °C/decade) and (d) the lower stratosphere (−0.29 °C/decade).

in a sufficient range). The "local slopes" were interpreted by fitting a straight line to $\log F_d(\tau)$ vs. $\log \tau$ within a small window and successively shifted over all calculated scales τ. However, to define the stability of the "local slopes" $a(\tau)$ vs. $\log \tau$, we applied the DFA method on 500 times series characterized by fractional Gaussian noise (i.e. Monte Carlo simulations) and we estimated the local slopes $a(\tau)$ vs. $\log \tau$ for each the 500 time series (Timmer and König, 1995). Then we determined a range $R = (\bar{a} - 2s_a , \bar{a} + 2s_a)$ where $\bar{a}$ and s_a denote the mean value and the standard deviation of the 500 estimated local slopes $a(\tau)$, correspondingly, over all scales τ.

3. Discussion and results

3.1. What the air temperature long-term trends actually show?

In this sub-section we investigate the air TA from the lower troposphere to the lower stratosphere in order to detect if there is any global warming signal.

Fig. 1 shows the trend of the air TA in the global lower troposphere (0.13 °C/decade), the global mid-troposphere (0.09 °C/decade), the global tropopause (0.01 °C/decade) and the global lower stratosphere (−0.29 °C/decade). All the trend values mentioned above are statistically significant (at 95% confidence level), except for tropopause, which can be assumed to be close to zero.

From Fig. 1 the pattern of the air TA trend shows that there is a decreasing warming from the lower troposphere up to the tropopause level (where it becomes zero) and then it reverts to a cooling in the lower stratosphere.

An identifiable signature of global warming is the combination of tropospheric heating and stratospheric cooling leading to an increase in the height of tropopause. However, according to Fig. 1 this is not the case, because the TA trend at the tropopause is near zero.

It should be of interest to see the latitudinal variation of the air temperature trend in both hemispheres. Table 1 shows the air TA trends as a function of height and latitude. Moreover, Table 2 presents the spatial variation characteristics of global air TA. The results depicted in Tables 1 and 2 are in close agreement with those recently published by Christy et al. (2018).

The following remarks can be drawn from Tables 1 and 2:

- In the lower stratosphere a decrease in the air TA is observed with a rate between 0.2 and 0.3 °C/decade, approximately. It should be noted that this cooling is lower over both poles (comparing with tropics and extratropics) with the lowest rate over the North Pole. It is worth to note that this result is consistent with the fact the ozone hole over the South Pole is larger than that over the North Pole.
- The tropopause air TA do not show any statistically significant trend, with the exception of the extratropics of the northern hemisphere where an increase is observed with a rate of 0.03 °C/decade.
- In the lower and mid-troposphere an increase in the air TA is recorded, except over the polar region of the southern mid-troposphere and lower troposphere, where a not significant cooling trend is observed. The trend varies between 0.06 and 0.25 °C/decade, which in general decreases with height.

Table 1
Air TA trends (in ^{0}C/decade) as a function of height and latitude (*with italics*: not statistically significant trends).

	NH-POL	NH-EXTR	TROPICS	SH-EXTR	SH-POL
Lower stratosphere	−0.19	−0.30	−0.29	−0.29	−0.26
Tropopause	*0.06*	0.03	*0.01*	*−0.005*	*−0.04*
Mid-Troposphere	0.19	0.13	0.08	0.06	*−0.01*
Lower Troposphere	0.25	0.18	0.12	0.09	*−0.002*

According to Hoskins (1991) the expectation for global warming is to be more enhanced at high latitudes near the surface. That is, in the case of global warming occurrence, warming would have been stronger at the poles and would gradually decrease by approaching the equator. However, the pattern depicted in Table 1 does not comply with the gradual increase of the warming with latitude as predicted by the global warming theory.

Therefore, it would be interesting to clarify whether the warming found in the global troposphere (except the region over the South Pole) is associated with the cooling detected in the global lower stratosphere, as predicted by the theory of global warming. A way to achieve this is to compare the intrinsic dynamics of the thermal regime of the troposphere with that of the lower stratosphere. This is accomplished in the next sub-section.

3.2. What does the noise of air temperature fluctuations reveal?

The anomalies of a parameter are usually considered as noise. Sometimes, however, the study of the noise reveals hidden features of the parameter under investigation.

The air temperature is a crucial thermodynamic parameter of the

Table 2
Spatial variation of the air TA trends (in ^{0}C/decade) from the lower troposphere to the lower stratosphere (*with italics*: not statistically significant trends).

	Lower Troposphere	Middle Troposphere	Tropopause	Lower stratosphere)
Globe Land/Ocean	0.18/0.11	0.13/0.08	0.02/*0.01*	*0.00*/−0.29
NH Land/Ocean	0.19/0.13	0.14/0.10	0.03/0.02	−0.30/−0.29
SH Land/Ocean	0.15/0.09	0.10/0.06	*−0.01/0.00*	−0.32/−0.29
Tropics Land/Ocean	0.16/0.11	0.11/0.08	*0.02/0.01*	−0.30/−0.29
NH-EXTR Land/Ocean	0.20/0.15	0.15/0.11	0.04/0.03	−0.30/−0.29
SH-EXTR Land/Ocean	0.14/0.08	0.08/0.05	*−0.03/0.00*	−0.33/−0.29
NH-POL Land/Ocean	0.23/0.28	0.17/0.21	*0.05/0.08*	−0.20/*-0.17*
SH-POL Land/Ocean	*0.08/-0.03*	*0.02/-0.03*	*−0.10/-0.01*	−0.35/−0.22

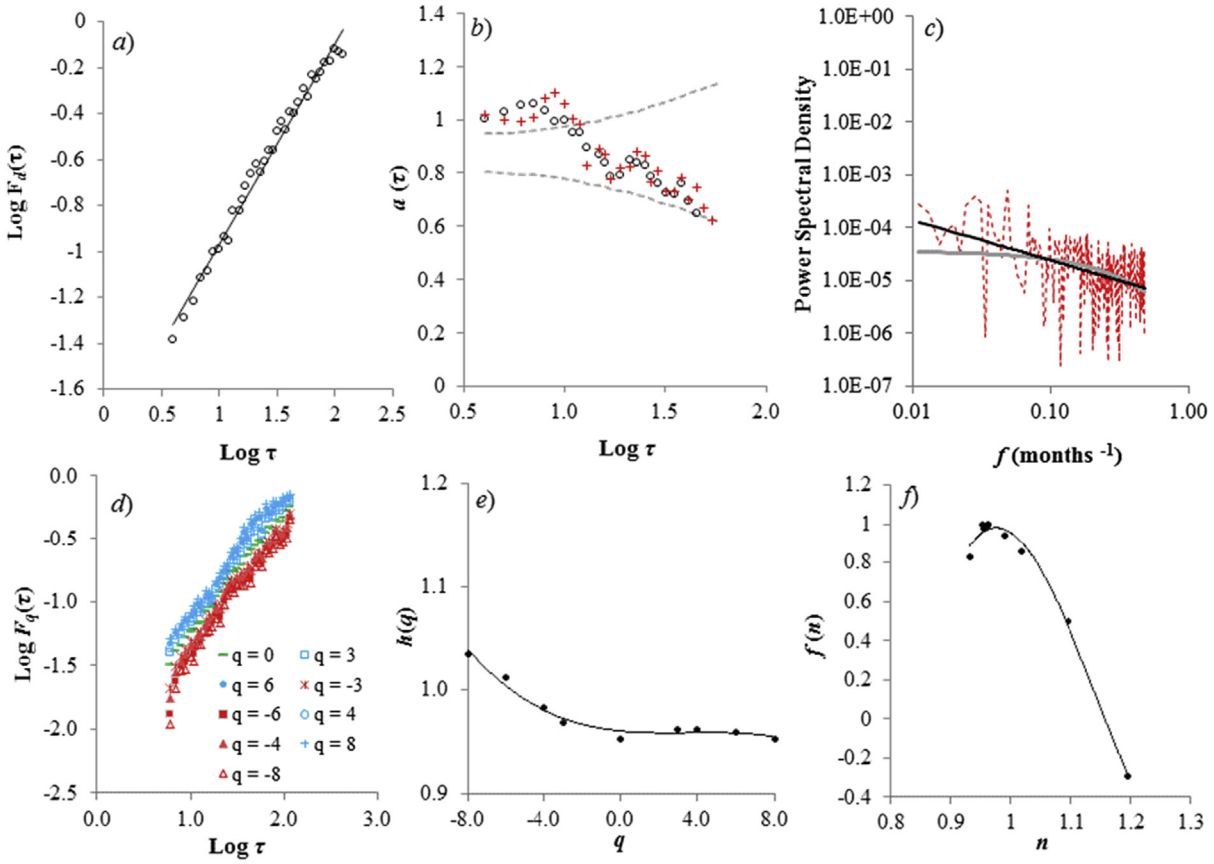

Fig. 2. *a*) Root-mean-square fluctuation function F_d (τ) (obtained from the DFA technique) vs. time scale τ (in months), in log-log plot, for the detrended and deseasonalised TA time series, over the global lower troposphere, during the period 12/1978–07/2018 with the corresponding linear fit (black line). *b*) Local slopes of the log$F_d(\tau)$ vs. logτ calculated within a window of 12 points (circles) and 10 points (crosses) for the time series described in (*a*). The dashed grey line indicates the corresponding $2s_a$ intervals around the mean value of the local slopes (mean α = 0.88). *c*) Power spectral density for the time series described in (*a*) with the corresponding power-law fit (black line) and the exponential fit (grey line). *d*) Log-log plots of the MF-DFA fluctuation factor $Fq(\tau)$ vs. the time scale τ of specific moments q for the for the time series described in (*a*). *e*) Generalized Hurst exponent $h(q)$ versus q-values, fitted by a third order polynomial. *f*) Singularity spectrum $f(n)$ versus singularity strength n, fitted by a third order polynomial.

atmosphere and plays an important role in the climate system. As mentioned in the introduction, the climate system is characterized by non-linear dynamics following the power-law variability. Therefore, it should be of interest to investigate the non-linear dynamics features of the temperature field of the troposphere and the lower stratosphere and to determine whether these are associated.

Fig. (2a) shows the root-mean-square fluctuation function $F_d(\tau)$ (extracted from the DFA technique) vs. time scale τ, in log-log plot, for the detrended and deseasonalised TA time series, over the global area of the lower troposphere, during the period 12/1978–07/2018. The corresponding best fit equation is $y = 0.88\times - 1.85$ (with $R^2 = 0.99$) giving a scaling exponent $a = 0.88 \pm 0.02$. However, in order to examine whether this value is statistically higher than 0.5 (which denotes white noise) we applied the DFA method to 500 time series characterized by the random noise (i.e. Monte Carlo simulations), in order to calculate the a-exponent. According to the Kolmogorov–Smirnov (Stephens, 1974) and Anderson–Darling (Anderson and Darling, 1954) best fit tests, the data set of the derived a-exponents obey the Gaussian distribution at 95% confidence interval with mean value $\bar{a}$ = 0.52 and standard deviation $s_a = 0.07$. So, the 95% confidence interval of $\bar{a}$ was $(\bar{a} - \frac{1.96}{\sqrt{500}}\cdot s_a, \bar{a} + \frac{1.96}{\sqrt{500}}\cdot s_a) = (0.51, 0.53)$ and the DFA exponent of the air TA time series (i.e. 088) is higher than the upper limit of this interval, revealing thus persistent features. In other words, the monthly mean fluctuations of the global air TA at the lower troposphere exhibit persistent long-range correlations, which means that small perturbations occurred in the past are closely and positively correlated with the later

on fluctuations with magnitude obeying power-law.

In order to verify these scaling properties, the two criteria proposed by Maraun et al. (2004) were tested. As derived from our analysis, the local slopes of $\log F_d(\tau)$ vs. $\log\tau$ depicted in Fig. (2b) (for two different window sizes of 10 and 12 points) lie within the boundary of the R range (after $\tau = 12$ months) and the profile of the power spectral density was better fitted by an hyperbolic (power law) curve (with equation $y = 4{\cdot}10^{-6}{\cdot}x^{-0.76}$ and $R^2 = 0.20$) than an exponential one (with equation $y = 4{\cdot}10^{-5}{\cdot}e^{-3.65x}$ and $R^2 = 0.13$) (Fig. (2c)).

Moreover, the hypothesis H_o: $R^2_{hyperbolic}$=$R^2_{\exp\ onential}$ vs. H_1: $R^2_{hyperbolic} \neq R^2_{\exp\ onential}$ was rejected using F-test (at 95% confidence level).

In addition, the MF-DFA technique applied to the above discussed time series revealed similar scaling features of $Fq(\tau)$ among all selected negative and positive moments. Exception to this rule was the case of the higher scales ($\tau > 35$) where the slope of $Fq(\tau)$ varies among the positive moments, as well as the case the smaller time scales ($\tau < 7$) where an increase of the slope of $Fq(\tau)$ was seen over the negative moments thus suggesting multifractality (Kantelhardt et al., 2002; Ihlen, 2012) (Fig. (2d)).

Furthermore, Figure (2e) depicts the empirical curve of $h(q)$ versus q fitted by the third order polynomial ($h(q) = -5{\cdot}10^{-5}q^3 + 0.0006q^2 - 0.002q + 0.96$, with $R^2 = 0.97$). The $h(q)$-values are much higher than 0.5, thus verifying the multifractality and the persistent long-range correlations of the time series considered. On the other hand, the slope and the values of $h(q)$ for the positive q-values are lower than the negative ones indicating features of multifractallity with different behavior for the moments of positive and negative signs.

Finally, Figure (2f) presents the empirical curve of singularity spectrum $f(n)$ (see the exact definition of $f(n)$ in Kantelhardt et al., 2002) versus singularity strength n fitted by the third order polynomial ($f(n) = 90.9n^3 - 312.3n^2 + 349.8n - 127.4$, with $R^2 = 0.99$). As shown, $f(n)$ displays a right tail indicating the lack of sensitivity for the large fluctuations, while the maximum value of $f(n)$ seemed to correspond approximately to $q = 0$. On the other hand, the n-values present a greater range on the right of $f(n)$ maximum (i.e., higher degree of multifractality for the negative q's), thus confirming the assumption of the Figure (2e).

The same conclusion is drawn from the DFA and MF-DFA analysis performed for the global air TA at the mid-troposphere and at the tropopause with a power-law exponent 0.98 ± 0.02 and 1.04 ± 0.01, respectively (see Table 3 and Figs. 3 and 4).

Consequently, the summarized conclusion form the DFA and MF-DFA analysis applied to the global troposphere (Table 3 and Figs. 2–4) is that the air TA fluctuations exhibit power-law persistent and multifractal behaviour with an exponent gradually increasing with altitude and maximized (to unity) at the tropopause for time-scales longer than about four months and shorter than about 6 years.

This result is consistent with the earlier findings by Efstathiou and Varotsos (2010) and by Varotsos et al. (2009)). It is interesting that the air TA of the global tropopause do not show any significant trend and is the center of the power-law behaviour following the 1/f fashion, which is the characteristic features of several geophysical parameters (e.g.Varotsos et al., 2003). In addition, the fact that the exponent α is close to unity, simply means that if the process is near Gaussian, there will probably be big low frequency fluctuations.

The cause of the $1/f$ behaviour (ι.e. the case of $\alpha = 1$) of several geophysical parameters is an open problem in the literature. The vertical distribution of α in the temperature fluctuations of the troposphere and lower stratosphere may be due to various mechanisms. It should be stressed that the exponent α is an indicator of the long-range correlations or the memory of the temperature field variability due to an external forcing. The higher the value of α, the stronger memory is. The maximum value of α is unity and then the memory is the highest possible. In the analysis presented above, the highest value of α ($\alpha \approx 1$) found at the level of the tropopause level. It is probably a result of either stronger positive feedbacks or greater inertia. So, the reduced slope α in the lower troposphere could be linked to the upward increase in climatic sensitivity due to the height-dependent feedbacks (Efstathiou and Varotsos, 2010).

The results obtained from the DFA and MF-DFA analysis of the global lower stratospheric air TA do not show any long-range correlation behaviour. Going in an in-depth analysis we study each latitude zone, separately. This shows that the low stratospheric TA over tropics obey power-law behaviour with an exponent 0.91 ± 0.02.

However, this is not the case for the low stratospheric temperature anomalies over both poles. This is probably due to the loss of the stratospheric ozone, which is largest in the lower stratosphere leading to a cooling of the austral polar vortex in springtime.

In this context, Wargan et al. (2018) analysing satellite data over the period 1998–2017 reported a negative ozone trend in the 10-km layer above the tropopause between 20°N and 60°N and a weaker one between 50°S and 20°S. In the tropics, they have found a positive trend is in a 5-km layer above the tropopause. They have attributed these trends to the enhanced isentropic transport between the tropical and extratropical lower stratosphere in the past two decades. This pattern in the low stratospheric ozone trend fits well to the presence of scaling of the air temperature anomalies over the tropics and its absence over extratropics and polar regions.

In addition, according to the results obtained by Xia et al. (2018) the upper troposphere and lower stratosphere are heated by ozone, which affects the high clouds (due to its effect on relative humidity) and the stratospheric water vapor (due to its impact on the tropical tropopause temperature). Consequently, the thermal regime in the lower stratosphere is mainly affected by the ozone dynamics in this area and not by the thermal regime in the troposphere alone. Therefore, the observed cooling in the lower stratosphere can not be attributed unambiguously to the warming of the troposphere, as dictated by the theory of global warming. This is a complicated and tricky issue due to various feedbacks involved.

Finally, due to the existence of very strong non-linear characteristics in temperature records, it was interesting to examine whether the application of different detrending methodologies would affect the results of DFA. Thus, by applying the DFA method to the detrended and deseasonalised air TA time series (over the global lower troposphere), the resulting a-exponent in the case of linear detrending was 0.89 ± 0.02, and 0.88 ± 0.02 (0.89 ± 0.02) in the case of polynomial detrending

Table 3
DFA and MF-DFA analysis applied to the detrended and deseasonalised TA time series, over the global mid-troposphere and tropopause, during the period 12/1978–07/2018.

	Mid-Troposphere	Tropopause
Linear fitting of $F_d(\tau)$ vs. τ	$y = 0.98x - 1.91$ and $R^2 = 0.99$	$y = 1.04x - 1.94$ and $R^2 = 0.99$
Power-law fit and exponential fit of the power spectral density	$y = 3{\cdot}10^{-6}{\cdot}x^{-1.04}$ with $R^2 = 0.30$ $y = 5{\cdot}10^{-5}{\cdot}e^{-5.03x}$ with $R^2 = 0.23$	$y = 2{\cdot}10^{-6}{\cdot}x^{-1.09}$ with $R^2 = 0.34$ $y = 6{\cdot}10^{-5}{\cdot}e^{-5.75x}$ with $R^2 = 0.26$
Third order polynomial of $h(q)$ vs. q	$h(q) = 3{\cdot}10^{-5}q^3 + 0.0007q^2 - 0.02q + 1.09$, *with* $R^2 = 1.00$	$h(q) = 5{\cdot}10^{-5}q^3 + 0.0007q^2 - 0.02q + 1.12$, with $R^2 = 1.00$
Third order polynomial of $f(n)$ vs. n	$f(n) = 6.47n^3 - 36.18n^2 + 56.32n - 25.78$, *with* $R^2 = 1.00$	$f(n) = 5.09n^3 - 29.95n^2 + 48.22n - 22.60$, with $R^2 = 0.99$

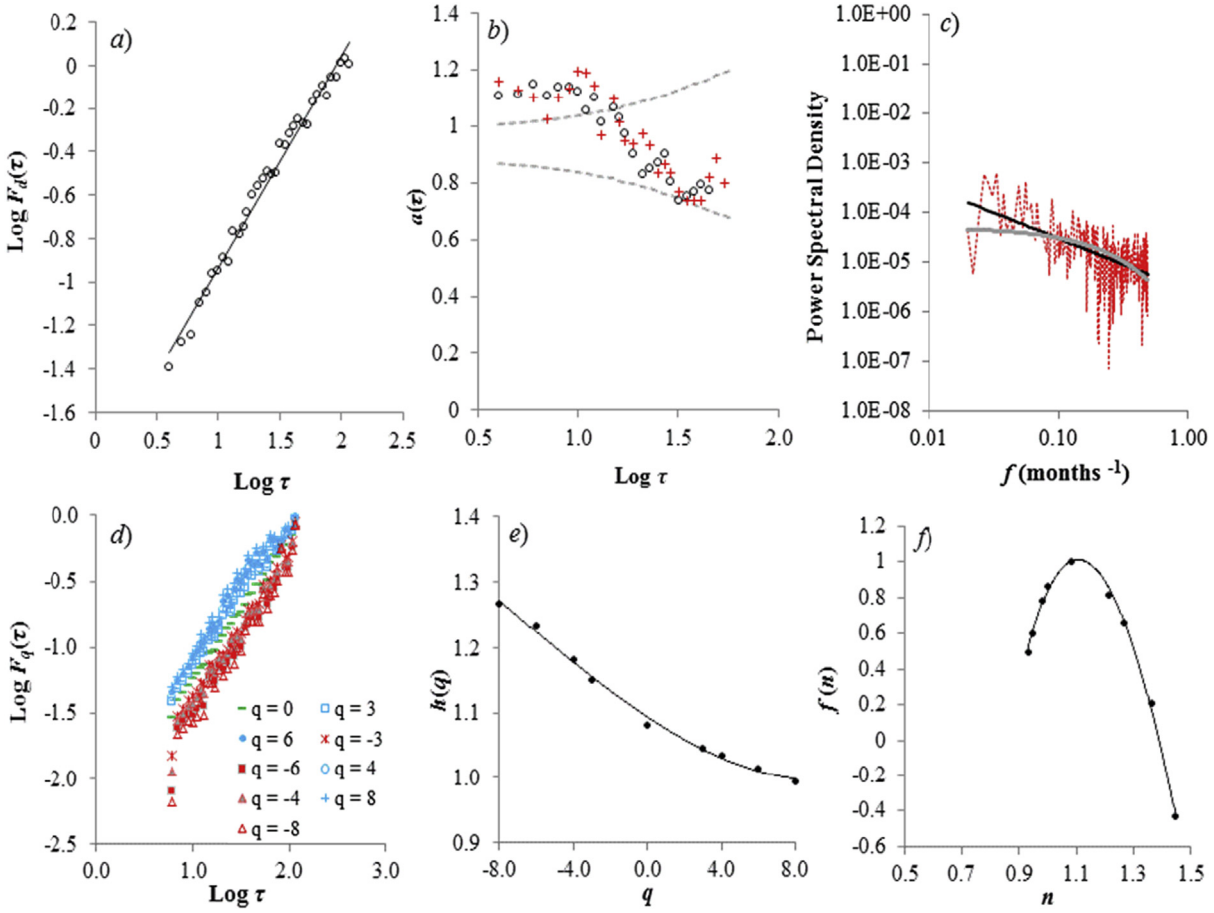

Fig. 3. *a*) Root-mean-square fluctuation function F_d (τ) (obtained from the DFA technique) vs. time scale τ (in months), in log-log plot, for the detrended and deseasonalised TA time series, over the global mid-troposphere, during the period 12/1978–07/2018 with the corresponding linear fit (black line). *b*) Local slopes of the log$F_d(\tau)$ vs. logτ calculated within a window of 12 points (circles) and 10 points (crosses) for the time series described in (*a*). The dashed grey line indicates the corresponding $2s_a$ intervals around the mean value of the local slopes (mean $\alpha = 0.95$). *c*) Power spectral density for the time series described in (*a*) with the corresponding power-law fit (black line) and the exponential fit (grey line). *d*) Log-log plots of the MF-DFA fluctuation factor $Fq(\tau)$ vs. the time scale τ of specific moments q for the for the time series described in (*a*). *e*) Generalized Hurst exponent $h(q)$ versus q-values, fitted by a third order polynomial. *f*) Singularity spectrum $f(n)$ versus singularity strength n, fitted by a third order polynomial.

of 6th degree (3^d degree). This indicates that the detrending methodology does not appear to statistically change the DFA results for the studied time series s. Furthermore, the MF-DFA technique is smoothing out such small differences in detrending tools.

4. Conclusions

From the analysis presented above the following conclusions could be drawn:

- The temperature trend shows a decreasing warming from the lower troposphere up to the tropopause level and then reverses to cooling in the lower stratosphere. This trend at the tropopause can be considered almost zero. The latter can not support the increase in the height of tropopause, a fingerprint of global warming.
- At the lower stratosphere there is a negative temperature trend which is lower over both poles (compared to tropics and extratropics) with the lowest value over the North Pole.
- In the lower and mid-troposphere the temperature trend decreases with height and latitude.

The above-mentioned three results do not agree with the global warming theory, namely, the gradual increase of tropospheric warming with latitude.

The DFA and MDFA analyses conducted on the possible association of warming in the global troposphere with cooling in the global lower stratosphere showed the following:

- The temperature fluctuations in the global troposphere exhibit power-law behaviour with an exponent gradually increasing with altitude reaching the unity at the tropopause.
- The global lower stratospheric temperature anomalies do not exhibit long-range correlation behaviour. In particular, the lower stratospheric temperature anomalies over tropics obey power-law behaviour, while it is not the case for the low stratospheric temperature anomalies over both poles. This may be attributed to the ozone dynamics in this region.

The two above-mentioned results lead to the main conclusion that the intrinsic properties of the thermal regime in the lower stratosphere are not associated with the thermal regime in the troposphere.

In summary, the tropospheric temperature has not increased over the last four decades, in both hemispheres, in a way that is more amplified at high latitudes near the surface. In addition, the lower stratospheric temperature did not decline as a function of latitude. Finally, the intrinsic properties of the tropospheric temperature are different from those of the lower stratosphere. Based on these results and bearing in mind that the climate system is complicated and complex with the existing uncertainties in the climate predictions, it is not possible to reliably support the view of the presence of global warming in the sense

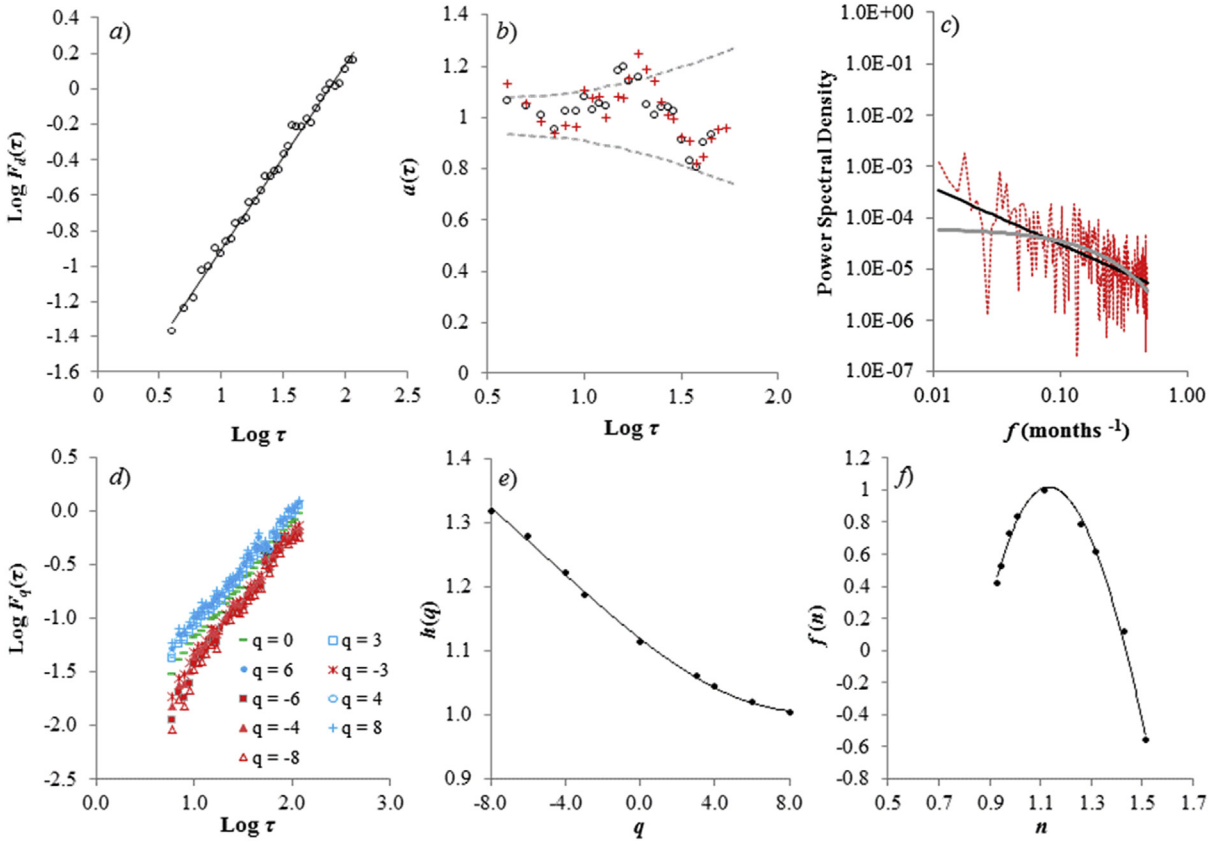

Fig. 4. *a*) Root-mean-square fluctuation function $F_d(\tau)$ (obtained from the DFA technique) vs. time scale τ (in months), in log-log plot, for the detrended and deseasonalised TA time series, over the global tropopause, during the period 12/1978–07/2018 with the corresponding linear fit (black line). *b*) Local slopes of the $\log F_d(\tau)$ vs. $\log\tau$ calculated within a window of 12 points (circles) and 10 points (crosses) for the time series described in (*a*). The dashed grey line indicates the corresponding $2s_a$ intervals around the mean value of the local slopes (mean $\alpha = 0.95$). *c*) Power spectral density for the time series described in (*a*) with the corresponding power-law fit (black line) and the exponential fit (grey line). *d*) Log-log plots of the MF-DFA fluctuation factor $Fq(\tau)$ vs. the time scale τ of specific moments q for the for the time series described in (*a*). *e*) Generalized Hurst exponent $h(q)$ versus q-values, fitted by a third order polynomial. *f*) Singularity spectrum $f(n)$ versus singularity strength n, fitted by a third order polynomial.

of an enhanced greenhouse effect due to human activities. The temperatures used are often estimated indirectly from satellite observations of radiances (e.g. Cracknell and Varotsos 2007, 2011). It would be interesting to directly analyse these radiances to answer questions about warming or cooling.

References

Anderson, T.W., Darling, D.A., 1954. A test of goodness of fit. J. Am. Stat. Assoc. 49 (268), 765–769.

Carleton, T.A., Hsiang, S.M., 2016. Social and economic impacts of climate. Science 353, aad9837. http://science.sciencemag.org/content/353/6304/aad9837.

Christy, J.R., Norris, W.B., Spencer, R.W., Hnilo, J.J., 2007. Tropospheric temperature change since 1979 from tropical radiosonde and satellite measurements. J. Geophys. Res. Atmos. 112 (D6). https://doi.org/10.1029/2005JD006881.

Christy, J.R., Spencer, R.W., Braswell, W.D., Junod, R., 2018. Examination of space-based bulk atmospheric temperatures used in climate research. Int. J. Remote Sens. 39 (11), 3580–3607.

Cracknell, A.P., Varotsos, C.A., 2007. Editorial and cover: Fifty years after the first artificial satellite: from Sputnik 1 to Envisat. Int. J. Remote Sens 28 (10), 2071–2072.

Cracknell, A.P., Varotsos, C.A., 2011. New aspects of global climate-dynamics research and remote sensing. Int. J. Remote Sens. 32 (3), 579–600.

Droegemeier, K.K., 2009. Transforming the sensing and numerical prediction of high-impact local weather through dynamic adaptation. Philos. Trans. A Math., Phys. Eng. Sci. 367 (1890), 885–904.

Efstathiou, M.N., Varotsos, C.A., 2010. On the altitude dependence of the temperature scaling behaviour at the global troposphere. Int. J. Remote Sens. 31 (2), 343–349.

Efstathiou, M.N., Varotsos, C.A., 2012. Intrinsic properties of Sahel precipitation anomalies and rainfall. Theor. Appl. Climatol. 109 (3–4), 627–633.

Efstathiou, M.N., Varotsos, C.A., 2013. On the 11 year solar cycle signature in global total ozone dynamics. Meteorol. Appl. 20 (1), 72–79.

Franzke, C.L., O'Kane, T.J., Berner, J., Williams, P.D., Lucarini, V., 2015. Stochastic climate theory and modeling. Wiley Interdisciplinary Reviews: Climatic Change 6 (1), 63–78.

Hoskins, B., 1991. A perspective on global warming. Renew. Energy 1 (1), 101–108.

Ihlen, E.A.F., 2012. Introduction to multifractal detrended fluctuation analysis in Matlab. Front. Physiol. 3, 141. https://doi.org/10.3389/fphys.2012.00141.

Intergovernmental Panel on Climate Change. Cambridge University Press: Cambridge, United Kingdom and New York, NY, USA, 2014.

Kantelhardt, J.W., Zschiegner, A., Koscielny-Bunde, E., Havlin, S., Bunde, A., Stanley, H.E., 2002. Multifractal detrended fluctuation analysis of nonstationary time series. Physica A 316, 87–114.

Kondratyev, K.Y., Varotsos, C., 1995. Atmospheric greenhouse effect in the context of global climate change. Il Nuovo Cimento C 18 (2), 123–151.

Lenton, T.M., Held, H., Kriegler, E., Hall, J.W., Lucht, W., Rahmstorf, S., Schellnhuber, H.J., 2008. Tipping elements in the Earth's climate system. Proc. Natl. Acad. Sci. U.S.A. 105 (6), 1786–1793. https://doi.org/10.1073/pnas.0705414105.

Lorenz, E., 1967. The Nature and Theory of the General Circulation of the Atmosphere. World Meteorological Organization, Geneva, Switzerland Publ. No. 218TP115.

Lovejoy, S., Varotsos, C., 2016. Scaling regimes and linear/nonlinear responses of last millennium climate to volcanic and solar forcings. Earth Syst. Dynam. 7 (1), 133–150.

Lucarini, V., 2011. Modelling Complexity: the Case of Climate Science. arXiv preprint arXiv:1106.1265.

Lucarini, V., Blender, R., Herbert, C., Ragone, F., Pascale, S., Wouters, J., 2014. Mathematical and physical ideas for climate science. Rev. Geophys. 52 (4), 809–859.

Maraun, D., Rust, H.W., Timmer, J., 2004. Tempting long-memory – on the interpretation of DFA results. Nonlinear Process Geophys. 11, 495–503.

Nambu, Y., 1973. Generalized Hamiltonian dynamics. Phys. Rev. D 7, 2403–2412.

OGorman, P.A., 2014. Contrasting responses of mean and extreme snowfall to climate change. Nature 512, 416. https://www.nature.com/articles/nature13625.

Peng, C.K., Buldyrev, S.V., Havlin, S., Simons, M., Stanley, H.E., Goldberger, A.L., 1994. Mosaic organization of DNA nucleotides. Phys. Rev. E 49 (2), 1685–1689.

Prigogine, I., 1961. Thermodynamics of Irreversible Processes. Interscience, New York.

Ruelle, D., 1997. Differentiation of SRB states. Commun. Math. Phys. 187 (1), 227–241.

Schleussner, C.-F., Donges, J.F., Donner, R.V., Schellnhuber, H.J., 2016. Armed conflict risks enhanced by climate-related disasters in ethnically fractionalized countries. Proc. Natl. Acad. Sci. Unit. States Am. 113, 9216–9221. http://www.pnas.org/

content/113/33/9216.
Stephens, M.A., 1974. EDF statistics for goodness of fit and some comparisons. J. Am. Stat. Assoc. 69 (347), 730–737.
Timmer, J., König, M., 1995. On generating power law noise. Astron. Astrophys. 300, 707–710.
Varotsos, C., 2002. The southern hemisphere ozone hole split in 2002. Environ. Sci. Pollut. Res. 9 (6), 375–376.
Varotsos, C., 2005. Power-law correlations in column ozone over Antarctica. Int. J. Remote Sens. 26, 3333–3342.
Varotsos, C.A., 2013. The global signature of the ENSO and SST-like fields. Theor. Appl, Climatol. 113 (1-2), 197–204.
Varotsos, C., Assimakopoulos, M.N., Efstathiou, M., 2007. Technical note: long-term memory effect in the atmospheric CO2 concentration at mauna loa. Atmos. Chem. Phys. 7, 629–634.
Varotsos, C.A., Efstathiou, M.N., Cracknell, A.P., 2013a. On the scaling effect in global surface air temperature anomalies. Atmos. Chem. Phys. 13 (10), 5243–5253.
Varotsos, C.A., Efstathiou, M.N., Cracknell, A.P., 2013b. Plausible reasons for the inconsistencies between the modeled and observed temperatures in the tropical troposphere. Geophys. Res. Lett. 40 (18), 4906–4910.
Varotsos, C., Cartalis, C., 1991. Re-evaluation of surface ozone over Athens, Greece, for the period 1901–1940. Atmos. Res. 26 (4), 303–310.
Varotsos, C., Efstathiou, M., Tzanis, C., 2009. Scaling behaviour of the global tropopause. Atmos. Chem. Phys. 9 (2), 677–683.
Varotsos, C.A., Cracknell, A.P., Efstathiou, M.N., 2018. The global signature of the el Niño/La Niña southern oscillation. Int. J. Remote Sens. 1–13. https://www.tandfonline.com/doi/full/10.1080/01431161.2018.1465617.
Varotsos, P.A., Sarlis, N.V., Skordas, E.S., 2003. Long-range correlations in the electric signals that precede rupture: further investigations. Phys. Rev. E 67 (2), 021109.
Wargan, K., Orbe, C., Pawson, S., Ziemke, J.R., Oman, L.D., Olsen, M.A., Coy, L., Knowland, K.E., 2018. Recent decline in extratropical lower stratospheric ozone attributed to circulation changes. Geophys. Res. Lett. 45 (10), 5166–5176.
Weber, R.O., Talkner, P., 2011. Spectra and correlations of climate data from days to decades. J. Geophys. Res. 106, 20131–20144.
Wiener, N., 1950. Extrapolation, Interpolation and Smoothing of Stationary Time Series. MIT Technology Press and John Wiley and Sons, New York.
Xia, Y., Huang, Y., Hu, Y., 2018. On the climate impacts of upper tropospheric and lower stratospheric ozone. J. Geophys. Res.: Atmosphere 123 (2), 730–739.